Crystal fields and microscopic local structures of some trigonal symmetry centres in fluorite crystals doped with trivalent rare-earth ions

1992 J. Phys.: Condens. Matter 4 1743

(http://iopscience.iop.org/0953-8984/4/7/012)

J. Phys.: Condens. Matter 4 (1992) 1743–1756. Printed in the UK

Crystal fields and microscopic local structures of some trigonal symmetry centres in fluorite crystals doped with trivalent rare-earth ions

K Leśniak† and F S Richardson‡

† Institute of Physics, Polish Academy of Sciences, Aleja Lotników 32/46, 02-668 Warszawa, Poland

‡ Department of Chemistry, University of Virginia, Charlottesville, VA 22901, USA

Received 4 September 1991

Abstract. Semi-empirical effective charge calculations were made of crystal field effects and the corresponding energy level splittings for NNN–F^- compensated centres in a number of RE^{3+}: fluorite structure systems. While the results obtained confirm that such centres were indeed observed in a number of experimental investigations of these dopant : lattice systems, in at least one instance (the *B* centre in the Er^{3+}: CaF_2 system) such identification appears to be untenable. Model reconstructions were also made of local lattice distortions in the centres in the Eu^{3+}: SrF_2 and Er^{3+}: SrF_2 systems. The two centres are structurally related but the corresponding local distortions appear to be qualitatively different, this result is discussed in the context of other recent work in the field. Finally, the procedure developed was used to improve the phenomenological calculation of B_q^k values for the trigonal centre in the Eu^{3+}: BaF_2 system, demonstrating its utility in such applications by significantly improving final fit quality.

1. Introduction

The presence of trigonal symmetry centres in alkaline-earth fluoride crystals doped with trivalent rare-earth (RE^{3+}) ions has been known for many years [1]. While some of these centres were thought to be associated with the charge-compensation of RE^{3+} ions by means of O^{2-} or OH^-, it has long been conjectured [2, 3], that one of the main types of site in this class was one in which the RE^{3+} dopant was associated with an interstitial F^- ion in a next-nearest-neighbour (NNN) position (figure 1).

Early work on the Er^{3+}: CaF_2 [4] and Er^{3+}: SrF_2 [5] systems appeared to confirm the presence of charge-compensated centres of this type, the results being consistent with the presence of centres with trigonal symmetry about the [111] direction. Moreover, the trigonal symmetry centres associated with F^- compensation were shown in a number of studies [5–10] to be progressively more important with increasing host lattice constant and RE^{3+} dopant mass.

The principal problem to be elucidated thus appeared to be establishing the point along the above sequence at which the trigonal centres start to appear in noticeable concentrations. In particular, the discussion focused on the structural identity of the trigonal symmetry site in the Er^{3+}: CaF_2 system, labelled the *B* site by Tallant and Wright [11]. Identification by Tallant and Wright of this site with the centre shown in figure 1

0953-8984/92/071743 + 14 $04.50

was questioned by other authors [8, 9]. Resolution of this controversy was all the more important for the fact that the tetragonal/trigonal (B) site ratio was shown [12] to decrease with increasing dopant concentration in the $Er^{3+}:CaF_2$ system and, thus, identification of the B site, with a centre as shown in figure 1, posed serious problems for simple defect equilibria pictures.

Recent studies of Cockroft *et al* [13, 14] have accentuated the above problems by confirming the trigonal symmetry of the B site, while questioning the model of the centre proposed by Tallant and Wright. This structural assignment of the B site was also recently challenged in the ENDOR study of Er^{3+} centres in CaF_2 and $KMgF_3$ by Grachev *et al* [15]. To add to the puzzle, Cockroft *et al* [14] also claimed noticeable deviations from trigonal symmetry for the dominant site in the $Er^{3+}:SrF_2$ system, labelled the J site by Kurz and Wright [16], and identified as a trigonal symmetry centre by Aizenberg *et al* [17].

The situation outlined above clearly called for an investigation of the structural identities of the various trigonal symmetry sites observed in the optical investigations of RE^{3+}: fluorite systems and their relation to the centre of figure 1. Such an investigation should, moreover, be more general than the purely experimental investigations of the energy level schemes of a given RE^{3+} ion (with their attendant problems of generalizing any conclusions to other dopants) or the purely phenomenological calculations of the crystal field parameters corresponding to the various sites (with the associated problem of identifying the spurious non-physical minima in the minimization procedure).

Previous work on the *a priori* prediction of the spectra of tetragonal symmetry sites in RE^{3+}: fluorite systems [18, 19] appeared to provide a model framework within which such an investigation could be conducted, and the present paper reports its results. Thus, in section 2 we outline the methods followed in linking the microscopic model of the centre of interest with the energy level schemes of the corresponding spectra. Following this, we discuss the identities of the various trigonal (or supposedly trigonal) sites in a number of RE^{3+}: fluorite systems and their relation to the centre of figure 1 (section 3). The following section (section 4) is devoted to an attempt to reconstruct the local lattice distortions in some trigonal centres. Finally, we apply the procedure developed to study a trigonal symmetry centre in the $Eu^{3+}:BaF_2$ system, where the absence of adequate data about the relevant cubic centre makes direct *a priori* energy level prediction impossible (section 5).

2. Model crystal field calculation

For a C_{3v} symmetry system (such as the centre of figure 1), the one-electron crystal field Hamiltonian takes the form [20]

$$H = B_0^2C_0^2 + B_0^4C_0^4 + B_3^4(C_{-3}^4 - C_3^4) + B_0^6C_0^6 + B_3^6(C_{-3}^6 - C_3^6) + B_6^6(C_{-6}^6 + C_6^6) \qquad (1)$$

with C_q^k being the usual spherical tensor operators and B_q^k the crystal field parameters.

We now follow the procedure adopted in previous studies [19, 21] (as well as in the three-parameter theory of crystal fields [22, 23]) and express B_q^k in the form

$$B_q^k = \tau^{-k}\langle r^k\rangle(1 - \sigma_k)A_q^k \qquad (2)$$

$\langle r^k\rangle$, τ, σ_k are, respectively, the relevant Hartree–Fock radial integral [24], an empirical factor correcting the inaccuracy of free-ion Hartree–Fock $\langle r^k\rangle$ values (as a result of both the inadequacy of the Hartree–Fock method and the 4f wave-function expansion in a

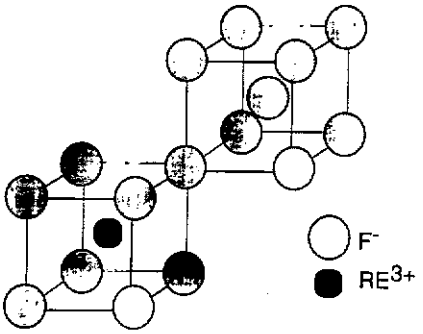

Figure 1. Local lattice structure of a NNN–F^- compensated centre in a RE^{3+}:fluorite system (local C_{3v} symmetry).

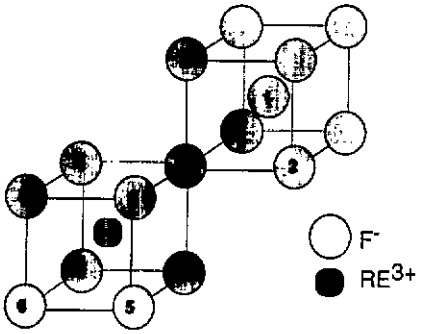

Figure 2. Relaxing F^- ions in a trigonal F^--compensated centre in a RE^{3+}:fluorite system. Assignments of the F^- ions to the various groups are indicated on the ions.

lattice environment), and the appropriate Sternheimer shielding factor (linearly extrapolated for the dopant of interest from the values of Erdos and Kang [25]).

The last quantity required to calculate B_q^k is the lattice sum A_q^k, given by

$$A_q^k = -\sum_i \frac{(Z_i e^2 Y_{kq}^*(\theta_i, \varphi_i))}{R_i^{k+1}} \tag{3}$$

with the summation index i running over all the lattice ions. In (3), $Z_i|e|$ and $(R_i, \theta_i, \varphi_i)$ are the charge and coordinates of ion i. As before [19, 21], the calculation of A_q^k is broken down into two parts, the lattice ions near the dopant being assigned effective charges and assumed to be displaced from their ideal lattice sites, while the rest of the lattice is modelled by fixed valence charges (i.e. Z_i is -1 or $+2$).

In the centre identification calculations reported in section 3, non-valence charges were assigned solely to the eight F^- ligands and the charge-compensating interstitial. As before [19], ligand effective charges Q_L and the value of τ were obtained from the phenomenological values of B_q^k for the cubic centre in the dopant:lattice system of interest. To do this, the ligands were assumed to move radially towards the dopant from their ideal lattice positions $\boldsymbol{d}_{1,i} = (1 - c)\,\boldsymbol{d}_{0,i}$, with the value of c obtained by requiring $|\boldsymbol{d}_{1,i} - \boldsymbol{d}_{0,i}|$ to be equal to the difference in the ionic radii of the host lattice cation and the dopant [26]. The resulting ligand positions $(R_i, \theta_i, \varphi_i)$ were then used to translate (by means of (2) and (3)) the two independent phenomenological B_q^k values for the cubic centre into the relevant values of Q_L and τ.

In the above, as well as the following calculations, the contribution to the value of A_q^k from the remainder of the lattice was obtained by subtracting from the lattice sums calculated for fluorite structure crystals by Vetri and Bassani [27], the lattice sum contribution due to the ions in the relaxation region (with the latter at their ideal lattice positions).

The effective charge $Q_I(r)$ of the F^- interstitial was obtained from an effective potential with Coulomb and Born–Mayer contributions

$$V(r) = Q_I(r)/r = Z/r + A\exp(-r/\rho) \tag{4}$$

using the procedure of [19]. For the centres of interest in this study (i.e. the dopant–

interstitial separations considered), the results differ little from those obtained by putting $Q_I(r) = -1.05$.

The values of Q_L, Q_I and τ obtained in this way, together with the positions $d_{1,i}$ of the nine F^- ions determined from the relation $d_{1,i} = (1 - c)d_{0,i}$, were used to calculate the values of the six non-vanishing B_q^k parameters (B_0^2, B_0^4, B_3^4, B_0^6, B_3^6, B_6^6) for the trigonal centre of interest.

Finally, the values of B_q^k were used to calculate the energy level splittings of a given dopant due to the crystal field in the centre investigated. The effects of intermediate coupling were accounted for in this calculation by using the reduced matrix elements of Carnall *et al* [28]. In the case of Eu^{3+}, the effects of J-mixing were taken into account by including the matrix elements between all the states of the ^7F term (with the barycentres of the ^7F J-multiplets being adjusted to correspond to their experimental values).

In some cases, where phenomenological B_q^k values for a trigonal centre were determined (and the centre was thought to be related to the centre of figure 1), attempts were also made to reconstruct the corresponding local lattice distortions. In these calculations, reported in section 4 of this paper, the relaxation region was taken to consist of 12 ions, these being the eight F^- ligands, the three F^- non-ligand ions closer to the dopant than the interstitial, and the interstitial itself (figure 2). The limited number of phenomenological values of B_q^k that formed the basis for this calculation, as well as symmetry constraints, made us group the relaxing F^- ions into six groups. The final positions of the ions in each group are arrived at by employing an independent relaxation parameter t_m ($m = 1, \ldots, 6$).

We were thus led to the following partition of the relaxing F^- ions (figure 2):

(a) Group 1: charge-compensating interstitial

$$d_{2,1} = d_{1,5} + t_1(d_{1,1} - d_{1,5})$$

(b) Group 2: three non-ligand F^- ions closer to the dopant than the interstitial

$$d_{2,i} = d_{1,5} + t_2(d_{0,i} - d_{1,5})$$

(c) Group 3: F^- ligand on the trigonal axis between the dopant and the interstitial

$$d_{2,5} = d_{0,1} + t_3(d_{1,5} - d_{0,1})$$

(d) Group 4: three F^- ligands closer to the interstitial

$$d_{2,i} = d_{1,5} + t_4(d_{1,i} - d_{1,5})$$

(e) Group 5: three F^- ligands further away from the interstitial

$$d_{2,i} = d_{1,5} + t_5(d_{1,i} - d_{1,5})$$

(f) Group 6: F^- ligand furthest from the interstitial

$$d_{2,12} = t_6 d_{1,12}$$

Extension of the relaxation region is, of course, inadvisable (there are only six independent phenomenological B_q^k) but the matter of further restricting it was felt to be worth pursuing. Thus, it was found that making t_1 and t_6 equal to unity throughout the simulation had no significant impact on model reproduction of phenomenological B_q^k values, as well as the values of t_m for the other relaxations. On the other hand, when only t_4 and t_5 were allowed to vary, their reconstructed values were close to those

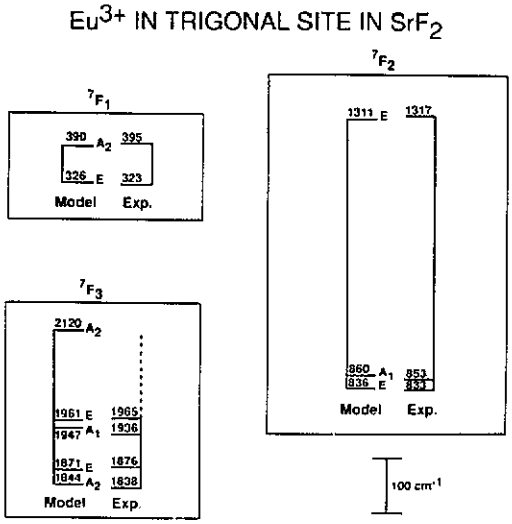

Figure 3. A comparison of model-predicted splittings of the $^7F_1$, $^7F_2$ and $^7F_3$ manifolds of Eu^{3+} in a NNN–F^- compensated site in SrF_2 with relevant experimental data on the trigonal symmetry centre collected by Jouart *et al* [30].

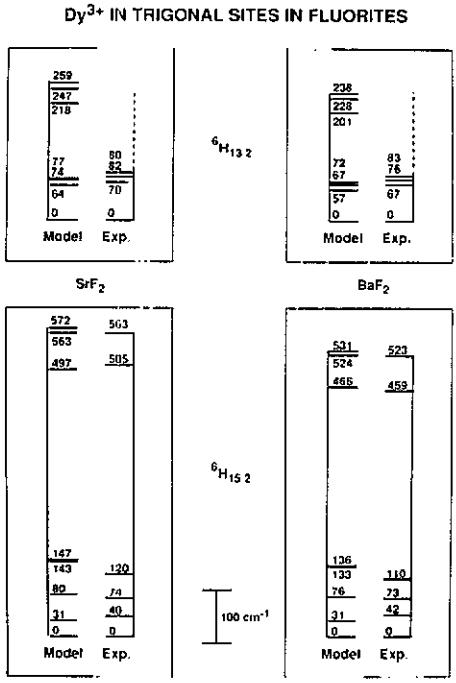

Figure 4. A comparison of model-predicted splittings of the $^6H_{15/2}$ and $^6H_{13/2}$ manifolds of Dy^{3+} in NNN–F^- compensated sites in SrF_2 and BaF_2 with relevant experimental data on the trigonal symmetry centres collected by Eremin *et al* [32].

obtained when all six t_m were allowed to change, although model reproduction of B_0^2 was poor. These effects stem from the fact that movements of ions in groups 4 and 5 have impact on all the B_q^k values, while those of the other ions significantly influence only some B_q^k. It is, however, important to underline that both groups 2 and 3 had to be included in the relaxation region before reasonably close reproduction of phenomenological B_0^2 could be achieved. This suggests that the ions in group 2 are far enough from the dopant for their positions to be determined mostly from B_0^2 values.

The above deduction has a direct bearing on the matter of reliability of model reproduction of local lattice relaxations. Previous work [29] suggests that such reproduction may be unrealistic for ions far from the dopant. This arises because such relaxations are determined almost solely from the values of B_q^k for $k = 2$ which also contain contributions from movements of ions outside the relaxation region. The fact that movements of the ions in group 2 (as well as those of the interstitial) are determined mostly from B_0^2 leads us to expect that model reconstruction of their positions may be physically unrealistic.

3. Trigonal centre identification

3.1. Europium

The spectrum of a trigonal symmetry centre was identified in the site-selective study of the Eu^{3+} : SrF_2 system carried out by Jouart *et al* [30]. The characteristic trigonal symmetry

splittings and the fact that the centre appears to be one of the major ones in this system suggest that it may be a NNN-compensated centre of figure 1.

Former work on the $Eu^{3+}:SrF_2$ system [19] provided values of the model quantities needed to test the above identification. We thus have $Q_L = -0.787|e|$, $\tau = 0.693$, $Z = -1.050$ and $A = 147.2$ for the system of interest, as well as $\rho = 0.5663$ for this and all the other dopant:lattice systems studied in this work (A and ρ in atomic units). Using the procedure outlined in section 2 these model parameter values give $B_0^2 = +192\,cm^{-1}$, $B_0^4 = +1350\,cm^{-1}$, $B_3^4 = -1580\,cm^{-1}$, $B_0^6 = +1220\,cm^{-1}$, $B_3^6 = +735\,cm^{-1}$, $B_6^6 = +771\,cm^{-1}$. The crystal field splittings of the $^7F_1$, $^7F_2$ and $^7F_3$ manifolds of Eu^{3+} corresponding to these B_q^k values are shown, and compared with the trigonal symmetry spectrum of Jouart *et al* [30], in figure 3. It is clear that the experimentally observed crystal field splittings are reproduced very closely, usually with accuracy better than $10\,cm^{-1}$. Clearly, the local lattice arrangement shown in figure 1 appears to be a good description of the lattice environment producing the observed level splittings.

We may note here that an apparently trigonal symmetry site was also observed in a site-selective study of the $Eu^{3+}:BaF_2$ system [31]. However, since the data on the cubic centre in this dopant:lattice system are insufficient for a crystal field analysis, direct model prediction of the trigonal centre splittings is, in this case, impossible. We shall return to this matter in section 5.

3.2. Dysprosium

Energy level splittings, as well as crystal field parameters, were reported for centres of trigonal symmetry in the $Dy^{3+}:SrF_2$ and $Dy^{3+}:BaF_2$ systems by Eremin *et al* [32]. Although not all the levels expected for the $^6H_{15/2}$ and $^6H_{13/2}$ manifolds were reported in that study, the data appear to be sufficient for a meaningful test of our model predictions.

The starting points of the present analysis were the crystal field parameters for cubic centres in these two systems obtained in previous work [21]. The values for the $Dy^{3+}:SrF_2$ system ($B_0^4 = -2029\,cm^{-1}$ and $B_0^6 = +654.8\,cm^{-1}$) correspond to $Q_L = -0.850|e|$, $\tau = 0.678$, $Z = -1.050$ and $A = 99.56$ (in atomic units). For the $Dy^{3+}:BaF_2$ system, the phenomenological crystal field parameter values of $B_0^4 = -1905\,cm^{-1}$, $B_0^6 = +590.4\,cm^{-1}$ reported in [21] correspond to $Q_L = -0.747|e|$, $\tau = 0.689$, $Z = -1.050$ and $A = 131.5$ (in atomic units). Using these model parameter values we obtain the following B_q^k values for the trigonal centres of interest (in cm^{-1}): $B_0^2 = +191$, $B_0^4 = +1370$, $B_3^4 = -1610$, $B_0^6 = +1160$, $B_3^6 = +700$, $B_6^6 = +734$ (SrF_2); $B_0^2 = +171$, $B_0^4 = +1290$, $B_3^4 = -1520$, $B_0^6 = +1050$, $B_3^6 = +632$, $B_6^6 = +663$ (BaF_2). The crystal field splittings of the $^6H_{15/2}$ and $^6H_{13/2}$ manifolds of Dy^{3+} corresponding to the above model values of B_q^k are shown, and compared with relevant experimental data, in figure 4. Again, we see that the model procedure followed led to a reasonably close reproduction of experimentally observed crystal field splittings. The results thus provide a basis for identifying the emission observed by Eremin *et al* [32] as arising from centres of the type shown in figure 1.

3.3. Erbium

As was noted in section 1 of this paper, structural identities of trigonal or supposedly trigonal sites in Er^{3+}:fluorite systems aroused particular interest in the past. In particular, this has been the case for a centre in the $Er^{3+}:CaF_2$ system labelled B by Tallant and

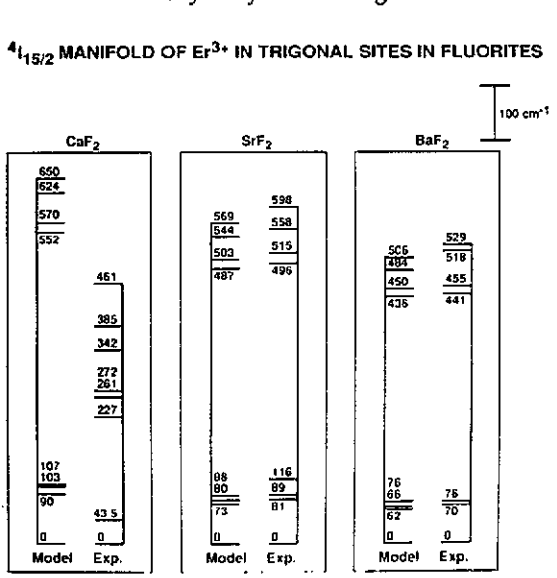

Figure 5. A comparison of model-predicted splittings of the $^4I_{15/2}$ manifold of Er^{3+} in NNN–F^- compensated sites in CaF_2, SrF_2 and BaF_2 with relevant experimental data on the *B* site [11], *J* site [14], and *L* site [16, 17], respectively.

Wright [11], for a long time thought to be a clear example of the centre shown in figure 1. However, more recent work [8, 9, 13–15] led a number of authors to question this identification, thus making the matter of the crystal field splittings that would be expected for a NNN-compensated site of trigonal symmetry in the $Er^{3+}:CaF_2$ system of special interest.

The starting points of the present attempt to address this question were the values of the model parameters established for the $Er^{3+}:CaF_2$ system in previous work [19]. These values ($Q_L = -0.800\ |e|$, $\tau = 0.662$, $Z = -1.05$ and $A = 109.0$ (in atomic units)) correspond to $B_0^2 = +218\ cm^{-1}$, $B_0^4 = +1290\ cm^{-1}$, $B_3^4 = -1510\ cm^{-1}$, $B_0^6 = +1160\ cm^{-1}$, $B_3^6 = +696\ cm^{-1}$, $B_6^6 = +730\ cm^{-1}$ for the centre shown in figure 1. The $^4I_{15/2}$ manifold splittings corresponding to above model values of B_q^k are shown, and compared with the experimentally observed *B* site splittings as found by Tallant and Wright [11], in figure 5.

Even a cursory glance at the above comparison reveals striking dissimilarities between the two energy level schemes being compared. Thus, the overall model-predicted splitting of the $^4I_{15/2}$ manifold (650 cm^{-1}) is very different from the corresponding quantity for the *B* site, as measured by Tallant and Wright [11], i.e. 461 cm^{-1}. Since all eight crystal field $^4I_{15/2}$ levels expected for a single ion site were observed by Tallant and Wright in the case of the *B* site, there appears to be little room for ambiguity in this matter. It is also apparent that the model splittings (which bear a clear relation to the splittings of the cubic centre in the $Er^{3+}:CaF_2$ system, with the cubic Γ_8 levels being slightly split) are very different from the *B* site splitting patterns. Indeed, it is quite clear that approximating the *B* site lattice arrangement by a slightly perturbed cubic centre is not a good point of departure for analysing the spectrum of this site.

We are thus led to concur with the authors who thought that the *B* site bears no direct relation (apart from symmetry) to the centre shown in figure 1. It may be noted in this context that alternative trigonal symmetry local lattice arrangements for RE^{3+}: fluorite systems have been discussed in the past [33].

The crystal field analysis of the cubic centre in the $Er^{3+}:SrF_2$ system reported in [21] allows us to perform an analogous simulation for this system. From the phenomenological values of B_q^k for the cubic centre ($B_0^4 = -1755\,cm^{-1}$, $B_0^6 = +567.4\,cm^{-1}$), we obtain $Q_L = -0.740\,|e|$, $\tau = 0.661$, $Z = -1.05$ and $A = 141.4$ (in atomic units) for the system of interest. For the centre shown in figure 1 in this dopant:lattice system we thus obtain: $B_0^2 = +197\,cm^{-1}$, $B_0^4 = +1190\,cm^{-1}$, $B_3^4 = -1390\,cm^{-1}$, $B_0^6 = +1010\,cm^{-1}$, $B_3^6 = +606\,cm^{-1}$, $B_6^6 = +636\,cm^{-1}$. In figure 5, the $^4I_{15/2}$ manifold crystal field splittings corresponding to the above B_q^k values are compared with the $^4I_{15/2}$ energy level scheme of the J site in the $Er^{3+}:SrF_2$ system [14]. The similarity of the above two energy level schemes is sufficiently close for us to identify the J site with a centre that appears to be structurally related to the centre shown in figure 1. We may, however, note that in some cases the divergence between the experimentally observed and calculated level energies is significantly larger (approximately $30\,cm^{-1}$) than was the case for the Eu^{3+} and Dy^{3+} centres analysed before.

In the case of the $Er^{3+}:BaF_2$ system, the primary candidate for the centre shown in figure 1 appears to be the site labelled L by Miller and Wright [34]. The phenomenological B_q^k values for the cubic centre in this dopant:lattice system ($B_0^4 = -1601\,cm^{-1}$, $B_0^6 = +504.6\,cm^{-1}$) [21] give $Q_L = -0.618\,|e|$, $\tau = 0.668$, $Z = -1.05$, $A = 172.2$ (in atomic units). For the centre shown in figure 1, we thus have the following model values of B_q^k: $B_0^2 = +179\,cm^{-1}$, $B_0^4 = +1080\,cm^{-1}$, $B_3^4 = -1270\,cm^{-1}$, $B_0^6 = +894\,cm^{-1}$, $B_3^6 = +539\,cm^{-1}$, $B_6^6 = +565\,cm^{-1}$. The $^4I_{15/2}$ manifold splittings resulting from these B_q^k values are shown, and compared with the L site splittings [16, 17], in figure 5. The agreement between the two energy level schemes appears to be close enough to claim that the NNN compensation arrangement of figure 1 provides a reasonably good description of the L site.

4. Local lattice distortions in trigonal centres

4.1. Trigonal centre in the $Eu^{3+}:SrF_2$ system

The results presented in section 3 indicate that in a number of cases the trigonal symmetry spectra observed in investigations of RE^{3+}:fluorite systems may, according to our model procedure, be identified as arising from the NNN-compensated centres of the type shown in figure 1. Cases where we may attempt to derive information about local lattice relaxations in these centres are, however, less numerous. The reason for this is the fact that reasonably reliable phenomenological B_q^k values are required for the centre of interest before simulation of local lattice distortions may be attempted. Thus, for example, the data on the Dy^{3+} centres analysed in section 3.3 appear to be too fragmentary for such a calculation to be really convincing.

From the foregoing discussion, it appears that the best choice for performing such a simulation is the trigonal centre in the $Eu^{3+}:SrF_2$ system. The close agreement between the experimental data and the model-predicted crystal field splittings reported in section 3 appears to remove the ambiguities of level identification for this centre, suggesting at the same time that phenomenological B_q^k values should not be too different from the model-predicted ones reported in section 3.

Using the latter model values as the starting values for a fitting procedure, the following phenomenological B_q^k values were obtained for the above trigonal centre in the $Eu^{3+}:SrF_2$ system: $B_0^2 = +239.4\,cm^{-1}$, $B_0^4 = +1504\,cm^{-1}$, $B_3^4 = -1528\,cm^{-1}$,

Table 1. Microscopic local structure of the trigonal centre of Eu^{3+} in SrF_2. R_i are dopant-F^- distances (au); R_1—ideal lattice, R_2—corresponding to $t_1 = 1.00$, $t_2 = 1.00$, $t_3 = 1.00$, $t_4 = 1.00$, $t_5 = 1.00$, $t_6 = 1.00$, R_3—final model reconstruction.

Group	RE^{3+}–F^- distance (au)			Final value of the relevant relaxation parameter
	R_1	R_2	R_3	
1	9.492	9.170	9.06	0.98
2	9.087	9.087	6.90	0.57
3	4.746	4.424	4.60	0.97
4	4.746	4.424	4.54	1.04
5	4.746	4.424	4.20	0.96
6	4.746	4.424	4.60	1.04

$B_0^6 = +970.4\,cm^{-1}$, $B_3^6 = +996.3\,cm^{-1}$, $B_6^6 = +924.9\,cm^{-1}$. These values reproduce the energy level splittings measured by Jouart *et al* [30] with an accuracy corresponding to $\sigma = 1.5\,cm^{-1}$ (figure 6). The simulation procedure outlined in section 2 of this paper was then used to reconstruct from the above phenomenological B_q^k values the structure of the emitting centre. In this simulation, the ligand charges were kept fixed at their Q_L values, while the charges of group 1 and group 2 ions were assumed to be dependent on their distance from the Eu^{3+} ion according to (4). Proceeding in this way, a minimum was found at $t_1 = 0.98, t_2 = 0.57, t_3 = 0.97, t_4 = 1.04, t_5 = 0.96, t_6 = 1.04$ that corresponds to model B_q^k values of: $B_0^2 = +235.1\,cm^{-1}$, $B_0^4 = +1529\,cm^{-1}$, $B_3^4 = -1591\,cm^{-1}$, $B_0^6 = +939.9\,cm^{-1}$, $B_3^6 = +883.3\,cm^{-1}$, $B_6^6 = +934.6\,cm^{-1}$. Model reconstruction of the structure of the centre of interest is shown in table 1.

In analysing the data in table 1, it should be remembered that the reconstructed distortions are superpositions of two types of relaxation—that due to the difference in the ionic radii of the dopant and the lattice cation, and that due to the processes associated with introduction of the interstitial. The first type of relaxation leads to a radial collapse of the lattice around the dopant, the dopant–ligand distances being reduced from $4.746\,a_0$ to $4.42\,a_0$ for the system of interest. In the second type of relaxation, the group 4 ligands are pushed away from the interstitial and the group 5 ions move closer to it; their final distances from the interstitial are thus, respectively, $4.54\,a_0$ and $4.20\,a_0$. Simultaneously, the separations between the dopant and the two F^- ligands on the trigonal axis increase, with the two ligands ending up as being equidistant from the dopant at $4.60\,a_0$. The unrealistically large movements of the group 2 ions towards the original position of the F^- ligand on the trigonal axis probably reflect the limited accuracy of determination of their positions that was underlined in section 2.

Comparing these movements with those established for the tetragonal centre in the same dopant : lattice system [19], we see that introduction of the interstitial appears to have a relatively greater impact on the lattice relaxation processes in the tetragonal centre in the Eu^{3+} : SrF_2 system, while the difference in the ionic radii of the dopant and the lattice cation is more significant for the trigonal centre. This is immediately apparent when the relaxation parameter values for the tetragonal centre in the Eu^{3+} : SrF_2 system [19], i.e. $t_1 = 1.01$, $t_2 = 1.18$, $t_3 = 0.75$, are compared with the t_m values determined above (with a note taken of the fact that the t_2 value for the trigonal centre is apparently a model artifact). This observation helps to explain why the *a priori* calculations of

section 2, in which the t_m values are, in effect, put equal to 1.00, have yielded crystal field splittings that are so close to experimental data.

It is difficult to obtain independent corroboration of the results of the above simulation of local lattice distortions in a trigonal centre since, unlike for the tetragonal centres, other calculations of local lattice relaxations in trigonal centres in RE^{3+}: fluorite systems are all but non-existent. The only calculation with which we can compare our results appears to be the superposition model estimate of lattice relaxation processes in the trigonal centre in the $Gd^{3+}:SrF_2$ system of Edgar and Newman [35]. In that study, it was estimated that, compared with their separations in the cubic centre in the $Gd^{3+}:SrF_2$ system, the group 4 ligands are pushed out by 1%, while the group 5 ions move towards the dopant by 2%. These appear to be close to our values, the data in table 1 showing the group 4 ligands being pushed out by 4% and the group 5 F^- ions moving towards the dopant by 4%. As far as the ions situated on the trigonal axis are concerned, Edgar and Newman surmise that the dopant moves towards the interstitial by 6.5% of the dopant–ligand separation in the cubic centre, with the two axial ligands moving so as to make their separations from the dopant unchanged. Our result of a 1% reduction in the dopant–interstitial separation is in accord with this picture but, for the reasons outlined in section 2, our reconstruction of movements of the interstitial must be viewed with caution. On the other hand, the prediction of our calculation of an increase in the dopant–axial ligand distance by 4% is in clear disagreement with the conclusions of Edgar and Newman. It is, however, interesting to note that our results agree with their assumption that the two axial ligands are equidistant from the dopant.

It is clear from the above discussion that at least some of the results of our reported simulations agree with conclusions of other investigators. A more definitive analysis cannot, however, be performed before more work is done in the field. Investigations of tetragonal centres in RE^{3+}: fluorite systems suggest that much useful data can be deduced from results of hyperfine interaction studies such as, for example, the study of trigonal centres in the $Er^{3+}:BaF_2$ system by Davituliani *et al* [36].

4.2. *Trigonal centre in the $Er^{3+}:SrF_2$ system*

The conclusions of section 3 are in clear accord with the traditional view that linked the *J* site of Kurz and Wright [16] with the NNN-compensated centre in the $Er^{3+}:SrF_2$ system. The purpose of the present discussion is thus to examine the conclusion of Cockroft *et al* [14] that the trigonal symmetry of the *J* site is not, in fact, exact.

We start by noting that from their analysis of the centre in question, Cockroft *et al* arrived at two sets of phenomenological crystal field parameter values; namely: (I) $B_0^2 = +189.0\,cm^{-1}$, $B_0^4 = +866.2\,cm^{-1}$, $B_3^4 = -1434\,cm^{-1}$, $B_0^6 = +1090\,cm^{-1}$, $B_3^6 = +698.4\,cm^{-1}$, $B_6^6 = +445.2\,cm^{-1}$ and (II) $B_0^2 = +189.0\,cm^{-1}$, $B_0^4 = +954.8\,cm^{-1}$, $B_3^4 = -1372\,cm^{-1}$, $B_0^6 = +1106\,cm^{-1}$, $B_3^6 = +675.4\,cm^{-1}$, $B_6^6 = +480.0\,cm^{-1}$. The difference between the two calculations was that the ground state *g*-values were included in the fit that led to set (II), and were disregarded in calculating (I). In further discussion we shall, however, concentrate on the information that may be derived from set (I), since our deductions based on both these B_q^k sets are qualitatively the same. Thus, the application of the lattice distortion simulation procedure of section 2 led to a minimum at $t_1 = 2.83, t_2 = 1.15, t_3 = 0.99, t_4 = 0.96, t_5 = 1.03, t_6 = 1.01$, corresponding to $B_0^2 = +194\,cm^{-1}$, $B_0^4 = +882\,cm^{-1}$, $B_3^4 = -1450\,cm^{-1}$, $B_0^6 = +1070\,cm^{-1}$, $B_3^6 = +538\,cm^{-1}$, $B_6^6 = +577\,cm^{-1}$.

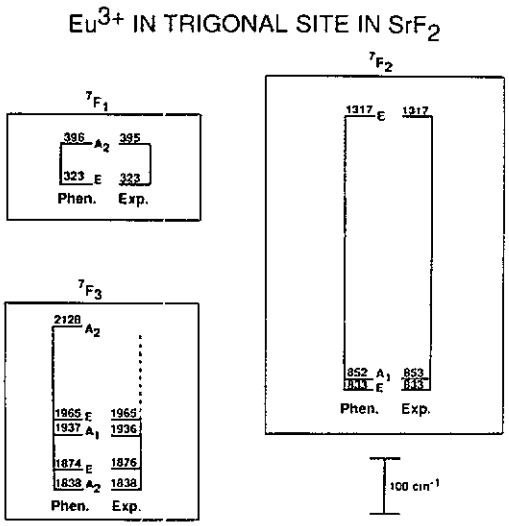

Figure 6. A comparison of experimental crystal field $^7F_1$, $^7F_2$ and $^7F_3$ splittings for the trigonal centre in the $Eu^{3+}:SrF_2$ system [30] with the splittings corresponding to phenomenological values of B_q^k.

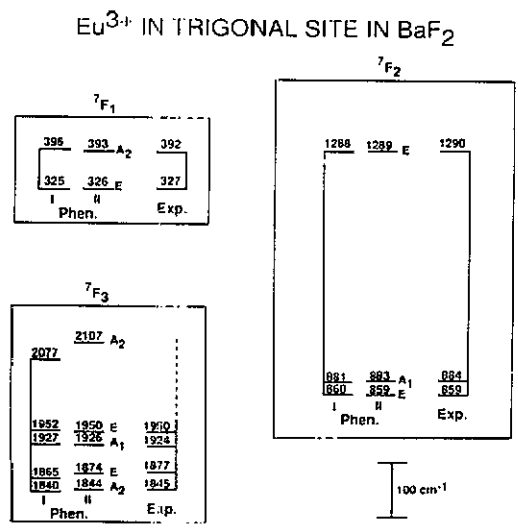

Figure 7. A comparison of experimental crystal field $^7F_1$, $^7F_2$ and $^7F_3$ splittings for the trigonal centre in the $Eu^{3+}:BaF_2$ system [31] with the splittings corresponding to phenomenological values of B_q^k. (I) and (II) correspond, respectively, to the first and second set of phenomenological B_q^k values (see text).

Comparing these results with those of the foregoing discussion of the trigonal centre in the $Eu^{3+}:SrF_2$ system, we see that the present simulation produced a picture of local lattice distortions very different from that presented in table 1. This is particularly significant in the case of t_4 and t_5 values since, as was noted in section 2, these are particularly insensitive to the details of the modelling procedure followed. Values of $t_4 = 0.96$, $t_5 = 1.03$ found for the *J* centre correspond to a situation in which group 4 ligands move towards the dopant, while group 5 ions are pushed out. This situation is the exact opposite to that found for the trigonal centre in the $Eu^{3+}:SrF_2$ system, where it was group 5 ions that moved towards the RE^{3+} ion and group 4 ligands that moved away. Moreover, the t_4 and t_5 values deduced from sets (I) and (II) are the same.

We thus conclude that while the NNN-compensation model provides a reasonable approximation to the structure of the *J* centre, its exact structure appears to be qualitatively different from that of the trigonal centre in the $Eu^{3+}:SrF_2$ system. It may, in particular, be the case that, as was concluded by Cockroft *et al*, the trigonal symmetry of the *J* centre is not exact.

5. Crystal field analysis of the trigonal centre in the $Eu^{3+}:BaF_2$ system

A well-known difficulty of any non-linear multiple-minima fitting problem is the fact that the choice of the starting point of the minimization procedure usually determines the quality and reliability of the final fit. This section contains a report of an attempt to employ the procedure outlined in section 2 to address this problem in the case of the crystal field splittings of a trigonal centre in the $Eu^{3+}:BaF_2$ system. The reason why the procedure employed in this case had to be different from, for example, that used in

fitting the splittings of Eu^{3+} in a trigonal site in SrF_2 was that the data on the cubic centres in the $Eu^{3+}:BaF_2$ system are, at present, insufficient for phenomenological B_q^k determination. Thus, a calculation in which B_q^k values corresponding to $t_m = 1.00$ are used as a starting point in fitting trigonal centre splittings is, at present, impossible for the $Eu^{3+}:BaF_2$ system.

There is, on the other hand, little reason to think that the trigonal centre observed by Jouart *et al* [31] in the $Eu^{3+}:BaF_2$ system is qualitatively different from the trigonal centre in the $Eu^{3+}:SrF_2$ system whose spectrum was reported in [30]. In accordance with theoretical calculations [7, 10] concerning the occurrence of NNN-compensated sites, the centre in question appears to be the dominant one in the $Eu^{3+}:BaF_2$ system. Moreover, the crystal field splittings in the trigonal centres in $Eu^{3+}:BaF_2$ and $Eu^{3+}:SrF_2$ systems are very similar. The above arguments are strong indications that the centre in question is thus the NNN-compensated centre of figure 1 that was analysed in the previous sections of this paper.

To start the calculation of phenomenological B_q^k values for this centre we therefore used the procedure followed in the centre identification calculations of section 3, with the ionic radii and lattice constant values appropriate to the $Eu^{3+}:BaF_2$ system, and the Q_L, τ, Z, A values determined previously for the $Eu^{3+}:SrF_2$ system. The resulting B_q^k values were: $B_0^2 = +178\,cm^{-1}$, $B_0^4 = +1550\,cm^{-1}$, $B_3^4 = -1830\,cm^{-1}$, $B_0^6 = +1360\,cm^{-1}$, $B_3^6 = +821\,cm^{-1}$, $B_6^6 = +861\,cm^{-1}$. Taking these values as the point of departure, we proceeded to fit the splittings in the trigonal centre in the $Eu^{3+}:BaF_2$ system observed by Jouart *et al*. The calculation resulted in phenomenological B_q^k values of $B_0^2 = +214\,cm^{-1}$, $B_0^4 = +1390\,cm^{-1}$, $B_3^4 = -1450\,cm^{-1}$, $B_0^6 = +811\,cm^{-1}$, $B_3^6 = +601\,cm^{-1}$, $B_6^6 = +623\,cm^{-1}$. These values reproduce the experimental crystal field splittings with an accuracy corresponding to $\sigma = 8.5\,cm^{-1}$ (figure 7). This value of σ is significantly larger than the $\sigma = 1.5\,cm^{-1}$ obtained in the analogous calculation for the $Eu^{3+}:SrF_2$ system, indicating that the initial B_q^k values do indeed seem to influence the quality of the final fit.

To improve on the starting point of the minimization procedure we employed a modified version of the distortion modelling procedure of section 4. In this calculation, the values of the distortion parameters t_m were fixed at the values previously determined for the trigonal centre in the $Eu^{3+}:SrF_2$ system; namely, $t_1 = 0.98$, $t_2 = 0.57$, $t_3 = 0.97$, $t_4 = 1.04$, $t_5 = 0.96$, $t_6 = 1.04$, and the quantities varied so as to reproduce the above phenomenological B_q^k values were the ligand effective charge Q_L and the wave-function expansion parameter τ. The sole minimum found in this way corresponds to $Q_L = -0.724\,|e|$, $\tau = 0.724$.

The above values of Q_L and τ were then used, together with $t_1 = 1.00$, $t_2 = 1.00$, $t_3 = 1.00$, $t_4 = 1.00$, $t_5 = 1.00$, $t_6 = 1.00$, to obtain what were hoped would turn out to be improved starting values of B_q^k for a phenomenological crystal field parameter determination for the system of interest. The starting B_q^k values obtained were $B_0^2 = +176\,cm^{-1}$, $B_0^4 = +1190\,cm^{-1}$, $B_3^4 = -1400\,cm^{-1}$, $B_0^6 = +967\,cm^{-1}$, $B_3^6 = +583\,cm^{-1}$, $B_6^6 = +611\,cm^{-1}$; a set noticeably different from that employed in the first phenomenological B_q^k determination.

The phenomenological B_q^k values obtained by fitting the experimentally measured splittings in the centre of interest starting from the above second set of initial B_q^k values were $B_0^2 = +225.0\,cm^{-1}$, $B_0^4 = +1275\,cm^{-1}$, $B_3^4 = -1428\,cm^{-1}$, $B_0^6 = +915.5\,cm^{-1}$, $B_3^6 = +856.6\,cm^{-1}$, $B_6^6 = +935.1\,cm^{-1}$. These values of crystal field parameters reproduce the experimental crystal field splittings with an accuracy corresponding to $\sigma = 2.4\,cm^{-1}$ (figure 7).

We thus see that the reported application of our modelling procedure helps to reduce significantly the deviation between the calculated and measured crystal field splittings (from $\sigma = 8.5\ cm^{-1}$ to $\sigma = 2.4\ cm^{-1}$), underlining its utility in analysing the spectra of trigonal centres in RE^{3+}: fluorite systems.

6. Conclusions

It is clear from the foregoing discussion that the modelling procedure outlined in this paper has indeed turned out to be a useful tool for tackling the problems presented in section 1. In particular, it has provided unequivocal support for linking some of the trigonal symmetry centres observed in optical investigations of RE^{3+}: fluorite systems with the NNN-compensation arrangements in figure 1. The selectivity of such identification may be seen in the case of the *B* centre in the $Er^{3+}:CaF_2$ system, where the present procedure clearly indicates that such identification is unwarranted, a view in accord with those of most other investigators. Furthermore, we were also able to obtain information about local lattice distortions in several centres of the type considered. Since this is, to our knowledge, the first instance when such a complete reconstruction of these distortions has been made for the centre type of interest, it is difficult to evaluate the quality of this reconstruction. We may, however, note that at least some of these results are in accord with a superposition model estimate performed by Edgar and Newman [35] for a trigonal centre in the $Gd^{3+}:SrF_2$ system.

The results of this study, as well as analogous work on the tetragonal [18, 19] and cubic [21] centres in RE^{3+}: fluorite systems give clear support to the view that a suitably modified electrostatic effective charge model may still be of some use in analysing rare-earth crystal field spectra. It should, however, be stressed in this context that such applications need to be judicious, with at least one example (the cubic centre in the $Eu^{3+}:PbF_2$ system [21]) clearly illustrating the limitations of such a model.

Finally, as was noted in [19], the approach advocated in this and preceding papers offers a clear path to tackling the problem of calculating the lattice sums A_q^k for odd k, and thus, ultimately, that of calculating the $f \rightarrow f$ transition probabilities.

Acknowledgments

The study whose results are reported in this paper was performed during the stay of one of the authors (KL) at the Department of Chemistry of the University of Virginia under a scientific exchange programme between the Polish Academy of Sciences and the US National Academy of Sciences. He would like to thank all the people who made this visit possible and all those whose hospitality and help has made it a fruitful one. Particular thanks are given to Dr P S May for his help with technical preparation of the figures for this paper. This work was also supported by a research grant from the US National Science Foundation (CHE-8820180).

References

[1] Baker J M 1974 *Crystals with the Fluorite Structure* ed W Hayes (Oxford: Clarendon)
[2] Ranon U and Yaniv A 1964 *Phys. Lett.* **9** 17

[3] Weber M J and Bierig R W 1964 *Phys. Rev.* **134** A1492
[4] Rector C W, Pandey B C and Moos H W 1966 *J. Chem. Phys.* **45** 171
[5] Brown M R, Roots K G, Williams J M, Shand W A, Groter C and Kay H F 1969 *J. Chem. Phys.* **50** 891
[6] Lenting B P M, Numan J A J, Bijvank E J and den Hartog H W 1976 *Phys. Rev.* B **14** 1811
[7] Catlow C R A 1976 *J. Phys. C: Solid State Phys.* **9** 1845
[8] Andeen C G, Fontanella J J, Wintersgill M C, Welcher P J, Kimble R J Jr and Matthews G E 1981 *J. Phys. C: Solid State Phys.* **14** 3557
[9] Kimble R J Jr, Welcher P J, Fontanella J J, Wintersgill M C and Andeen C G 1982 *J. Phys. C: Solid State Phys.* **15** 3441
[10] Corish J, Catlow C R A, Jacobs P W M and Ong S H 1982 *Phys. Rev.* B **25** 6425
[11] Tallant D R and Wright J C 1975 *J. Chem. Phys.* **63** 2074
[12] Moore D S and Wright J C 1981 *J. Chem. Phys.* **74** 1626
[13] Cockroft N J, Thompson D, Jones G D and Syme R W G 1987 *J. Chem. Phys.* **86** 521
[14] Cockroft N J, Jones G D and Syme R W G 1990 *J. Chem. Phys.* **92** 2166
[15] Grachev V G, Zaripov M M, Ibragimov I R, Rodionova M P and Falin M L 1989 *Sov. Phys.–Solid State* **31** 82
[16] Kurz M D and Wright J C 1977 *J. Lumin.* **15** 169
[17] Aizenberg I B, Livanova L D, Saitkulov I G and Stolov A L 1969 *Sov. Phys.–Solid State* **10** 1595
[18] Leśniak K 1988 *J. Opt. Soc. Am.* B **5** 1266
[19] Leśniak K 1991 *J. Chem. Phys.* **94** 3919
[20] Wybourne B G 1965 *Spectroscopic Properties of Rare Earths* (New York: Wiley Interscience)
[21] Leśniak K 1990 *J. Phys.: Condens. Matter* **2** 5563
[22] Karayianis N and Morrison C A 1975 *Harry Diamond Laboratories Report* No TR-1682
[23] Leavitt R P, Morrison C A and Wortman D E 1975 *Harry Diamond Laboratories Report* No TR-1673
[24] Freeman A J and Watson R E 1962 *Phys. Rev.* **127** 2058
[25] Erdos P and Kang J H 1972 *Phys. Rev.* B **6** 3393
[26] Tennent R M (ed) 1974 *Science Data Book* (Edinburgh: Oliver and Boyd)
[27] Vetri G and Bassani F 1968 *Nuovo Cimento* B **55** 504
[28] Carnall W T, Crosswhite H and Crosswhite H M 1977 *Argonne National Laboratory Special Report*
[29] Lésniak K 1986 *Acta Phys. Polon.* A **69** 473
[30] Jouart J P, Bissieux C, Mary G and Egee M 1985 *J. Phys. C: Solid State Phys.* **18** 1539
[31] Jouart J P, Bissieux C and Mary G 1987 *J. Lumin.* **37** 159
[32] Eremin M V, Luks R K and Stolov A L 1971 *Sov. Phys.–Solid State* **12** 2820
[33] Welsh H K 1985 *J. Phys. C: Solid State Phys.* **18** 5637
[34] Miller M P and Wright J C 1978 *Phys. Rev.* B **18** 3753
[35] Edgar A and Newman D J 1975 *J. Phys. C: Solid State Phys.* **8** 4023
[36] Davituliani A, Kiknadze M, Mirianashvili R and Sanadze T 1987 *Phys. Status Solidi* b **140** K69